Thermochimica Acta 478 (2008) 28–33

Contents lists available at ScienceDirect

Thermochimica Acta

journal homepage: www.elsevier.com/locate/tca

High-temperature oxidation of precipitation hardening steel

G. Vourlias, N. Pistofidis, K. Chrissafis*

Department of Physics, Aristotle University of Thessaloniki, 541 24 Thessaloniki, Greece

ARTICLE INFO

Article history:
Received 5 May 2008
Received in revised form 24 July 2008
Accepted 12 August 2008
Available online 28 August 2008

Keywords:
Steel
Oxidation
Scanning electron microscopy (SEM)
X-ray diffraction (XRD)
Thermo-gravimetric analysis (TGA)

ABSTRACT

The oxidation of precipitation hardening (PH) steels is a rather unexplored area. In the present work an attempt is made to estimate the oxidation mechanism and the kinetics for a PH steel. For this purpose specimens of the material under examination were isothermally heated at 850, 900 and 950 °C for 15 h. The as-treated samples were examined with SEM and XRD, while kinetics was based on TGA results. From this examination it was deduced that a thick scale is formed on the substrate surface, which, regardless the oxidation temperature, is composed by different oxides arranged in the form of successive layers. Of course the distribution in the different layers is not uniform but the oxides of the minor elements tend to be gathered at certain layers. The layer close to the substrate is compact while the upper layer seems more porous. Regarding kinetics, the mathematical analysis of the collected data shows that the change of the mass of the substrate per unit area vs time is described by a parabolic law. Hence oxidation is impeded as the exposure time increases.

1. Introduction

The oxidation of steel at high temperature is a very common phenomenon. In general, the mechanism which is responsible for this physico-chemical transformation could be divided in two stages, following the oxidation rate (e.g. the mass change of the oxides formed with regard to the exposure time in the aggressive environment): an initial stage, where the rate of oxidation is linear and a subsequent stage, where the rate of oxidation follows a parabolic low [1–3].

The linear behavior lasts for a short period of time up to the formation of a thin oxide layer. The actual rate observed in this stage depends on the oxidizing species. It is also controlled either by the rate of chemical reactions taking place at the scale–gas interface or by the rate of transport of the oxidizing species through the gaseous phase to the reaction surface. The former is usually interpreted in terms of adsorption rate of the oxidizing species on the scale surface and the incorporation of atomic oxygen into the oxide layer.

When the scale reaches a certain thickness, between about 4×10^{-3} and 0.1 mm, as found by Pettit and Wagner [4], the oxidation mechanism changes and the oxidation rate starts being controlled by the diffusion of ionic species through the oxide layer (and not through the gaseous phase). As a result, the growth rate of the scale is a parabolic function of the exposure time. Wagner [5] assumed that parabolic oxidation is strictly driven by the diffusion of metal ions and vacancies through the scale and that the chemical equilibrium at the metal–oxide and oxide–gas interfaces is maintained during the course of oxidation. Studies on the self-diffusion coefficient of iron in iron oxides [6,7] have shown that the growth of iron oxides is driven by cationic diffusion of iron ions, in accordance with the Wagner's postulations.

Kofstad [8], in order to describe mathematically the iron oxidation in oxygen, took for granted that oxygen adsorption and the incorporation of oxygen atoms into the oxide are the rate-controlling steps. However, his expression has only been confirmed for the case of low-pressure oxidation of niobium and tantalum in the temperature range 1000–1600 °C [9,10]. Later studies [11–13] have shown that at the initial rate of oxidation of iron with gas mixtures of oxygen and nitrogen, up to 3% of oxygen is controlled by the rate of oxygen transport to the reaction surface.

This short review shows that the high-temperature oxidation of steel has been studied extensively, along with the properties of the oxides formed on steel surfaces. A large part of these experimental and theoretical studies has dealt with the oxidation in CO—CO_2 mixtures at various temperatures [14–19], while the effect of oxygen and air (humid or moist) has also been investigated in detail [1–3].

However, all the above-mentioned studies, while very accurate and detailed, are focused on traditional alloys. Modern alloys have not been adequately examined in so many details. A typical material of this kind is the precipitation hardening (PH) steel which is examined in the present work. Its chemical composi-

* Corresponding author. Tel.: +30 2310 998188; fax: +30 2310 998188.
E-mail address: hrisafis@physics.auth.gr (K. Chrissafis).

0040-6031/$ – see front matter © 2008 Elsevier B.V. All rights reserved.
doi:10.1016/j.tca.2008.08.006

Table 1
Typical analysis of the examined steel

Element	wt.%
C	0.03
Si	0.3
Mn	6.3
Cr	12.0
Mo	1.4
Al	1.6

tion is reported in Table 1. This is a new composition that was recently formulated. The chemical analysis of the substrates was accomplished by the manufacturer with mass spectrometry. The main characteristic of this steel is that its mechanical properties (strength, superficial hardness and stiffness) are developed after a certain thermal treatment [20]. This property constitutes the most important advantage of these alloys, since they can be easily machined to the desirable form before precipitation, while they are still ductile. As a result they are suitable for the construction of complicated forms, such as injection moulds for plastics and rubber.

Consequently, in the present work an attempt is made to clarify the oxidation mechanism of a PH steel through a combined study of reaction kinetics, and morphology and chemical composition of the oxides formed. More specifically, kinetics is used for the evaluation of the growth of the scale. In this case the initial stage of oxidation is of importance, because it could reveal the phenomena that trigger oxidation. As a result, data could be gathered for the effective protection of the substrate. Furthermore, the evaluation of the parabolic oxidation rate constants under the conditions of the experiments offers information about the durability of the examined material in the aggressive environment and thus enable an accurate estimation of the service life of the steel under investigation.

2. Experimental

The substrates used were machined in rectangular specimens with dimensions 5 mm × 3 mm × 2 mm, while their surface was well-polished up to 5 μm alumina emulsion. Their oxidation took place in a TG-DTA Setaram Setsys 16/18 in alumina crucibles in an O_2 atmosphere with a 50-ml/min gas flow and heating rate 1 °C/min, from ambient temperature up to 1000 °C. Isothermal measurements were done for three different temperatures, 850, 900 and 950 °C in O_2 atmosphere, while the non-isothermal step before this took place in Ar atmosphere. TG-DTA allowed also the quantitative estimation of oxidation, while the continuous recording of mass, temperature and time allowed the on-line monitoring of the oxidation phenomena. As a result, accurate measurements over a long period of time were recorded and, therefore, an accurate determination of oxidation kinetics in their integral or derivative form was calculated.

The morphology and the chemical composition of the oxidation products was determined with scanning electron microscopy (SEM) using a 20-kV JEOL 840A SEM equipped with an OXFORD ISIS 300 EDS analyzer and the necessary software to perform point microanalysis, linear microanalysis and chemical mapping of the surface under examination. For the SEM examination, the surface of the samples did not undergo any preparation and the examination was direct, while for the examination of the cross-section segments have been cut from each sample, mounted in Bakelite, and polished down to 5 μm alumina emulsion.

3. Results and discussion

3.1. Initial considerations

For the determination of the temperatures used for this study, the substrate under examination was initially heated with a rate of 1 °C/min up to 1000 °C in pure oxygen. From this procedure it was deduced that oxidation till 700 °C is negligible, as the mass change shows. After this temperature the oxidation rate is very low. At about 800 °C the rate increases faster, while after 880 °C the slope of the plot becomes much steeper.

From this analysis it could be concluded that the isothermal study would be more efficient if the temperature chosen was above 800 °C, where oxidation is more intense, as it was already mentioned. For this reason it was finally decided to study oxidation at 850, 900 and 950 °C. Furthermore, in order to avoid the effect of the non-isothermal stage, where inevitably the temperature would be below the chosen target, the initial heating took place in an argon atmosphere. Oxygen was introduced in the system only after the achievement of the target-temperature.

3.2. Examination with SEM

The samples after the isothermal treatment were examined with SEM. After prolonged exposure (about 15 h) at 850 °C (Fig. 1a), the superficial appearance of the substrate varies. Small and rather smooth crystals seem to grow and cover the substrate. These crystals are not evenly distributed on the steel, but they form a morphological surface pattern composed by areas with different heights. As a matter of fact, they seem to form flower-like clusters.

The exposure of the substrates at different temperatures causes also a differentiation of the scale appearance. At 900 °C, after 15 h in the aggressive environment, the scale surface is more homogeneous. Larger crystals with different shapes are observed. Apart from smooth, rounded formations that cover the majority of the surface, large, angular crystals are also scattered. At 950 °C, after the same heating period, the angular crystals are absent and only smooth formations are present (Fig. 1b), which result in a surface that looks like a living tissue.

The examination of the cross-section prepared for samples treated at different temperatures and after same exposure period offers new informations. As Fig. 2 shows, the scale is separated in four layers. The lower one is compact, while the bigger upper one remains porous. These two zones are not in contact but they are separated by a thin layer. This layer is distinguished by its lighter hue. As it is expected, the scale thickness increases with regard to the oxidation temperature. In a similar way, the thickness of each layer that composes the scale increases.

From these micrographs it is clear that the superficial formations which are presented in the micrographs of Fig. 1, are not as compact as they seem. By contrast, voids at rather high density are observed in their mass. However, these voids do not form a continuous network that could facilitate diffusion of oxygen and thus oxidation.

The chemical composition of the scale could be determined with EDS. The results for the cross-sectional analysis are summarized in Fig. 3. XRD was also used [21], although only some speculations have been made based on this data, as the recorded peaks are only a few and they coincide for several different oxides. Fig. 3 shows that the cross-section of the samples is composed by different subscales. As a result, a multi-layered morphology prevails, as it was already observed. In each layer different compositions could be assigned, with regard to the stoichiometry or to the present

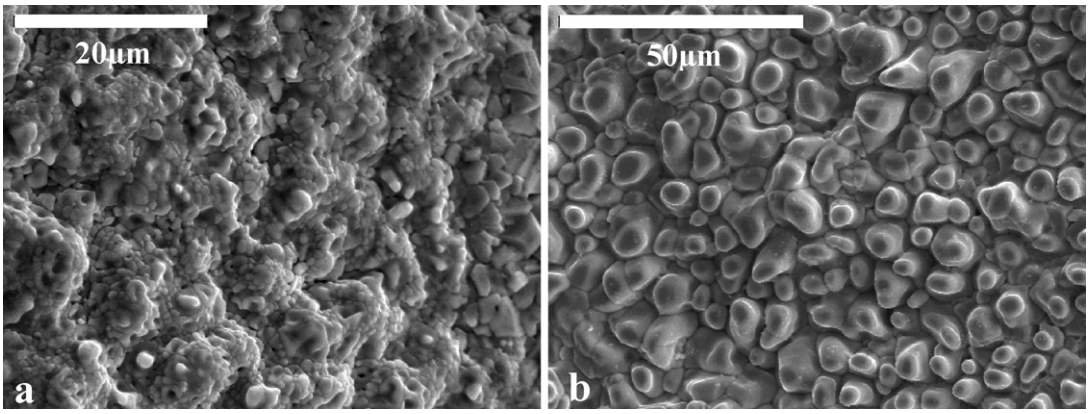

Fig. 1. Plane view of the oxidized steel after 15 h of exposure (a) at 850 °C and (b) at 950 °C.

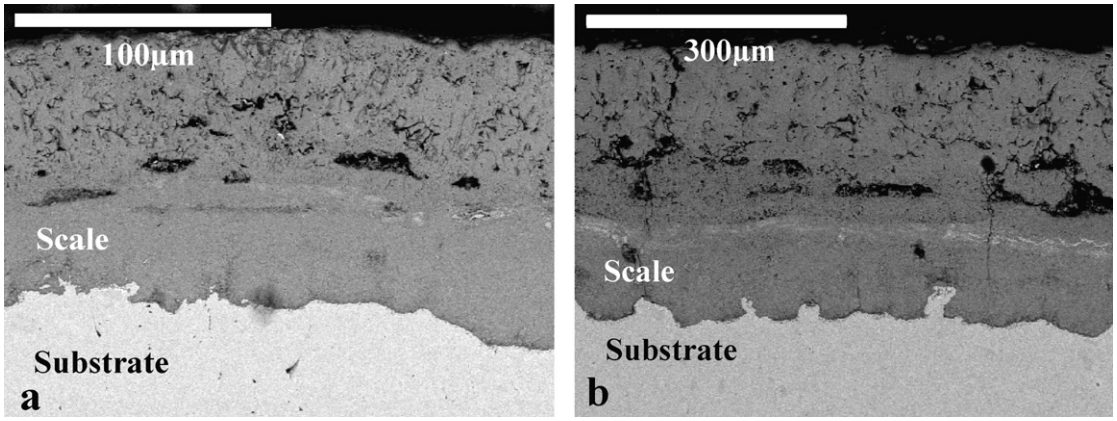

Fig. 2. Cross-section of the oxidized steel after 15 h of exposure (a) at 850 °C and (b) at 950 °C.

elements. The uneven distribution is due to the different diffusion coefficients of each element [21]. The above observations are more or less the same regardless the temperature. Of course the growth of the scale is faster as the temperature increases, since the physico-chemical reactions of oxidation proceed faster at higher temperatures.

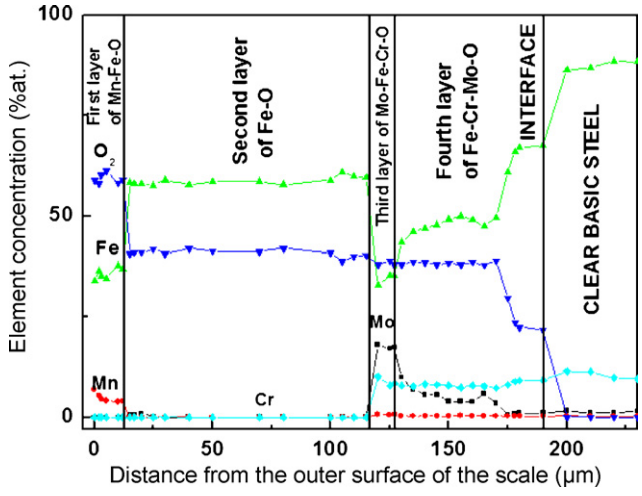

Fig. 3. Results of the EDS analysis along the cross-section of the scale formed at 900 °C after 15 h of exposure.

3.3. Theoretical background

The SEM examination offers much information. However, the conclusions are only qualitative. For the quantitative estimation of the performance of a material in an oxidizing environment a mathematical model is necessary. For this purpose, the most efficient way is to consider that the mass gain Δm due to oxidation is a function of the exposure time t in the aggressive environment, while the rest of the factors affecting the phenomenon are incorporated in a constant k_p. Hence, the comparison of the performance is reduced to the determination of the function that binds Δm and t along with the calculation of the constant k_p.

For the oxidation of a metallic material, it is usually considered that kinetics obeys a parabolic law. Hence, the weight gain per unit area can be expressed as follows:

$$\Delta m^2 = k_p t \quad (1)$$

where Δm is the mass gain per unit area at time t and k_p is the rate constant.

However, oxidation kinetics of only a limited number of pure metals and binary alloys might be described by this simple form of the parabolic law. As it is already mentioned, for the majority of metallic materials, particularly for complex alloys (such as the alloy under examination), the parabolic rate is generally established only after an initial transient oxidation faster kinetics according to a different law or rate constant. For this reason the parabolic rate kinetics is also referred to as the steady state kinetics. Depending on the specific oxidation behavior, the law describing the oxidation

of complex alloys could be stated as following:

$$\Delta m^2 = k_p(t - t_i) \quad (2)$$

or

$$(\Delta m - \Delta m_i)^2 = k_p t \quad (3)$$

where Δm_i refers to the initial weight-gain after the period of time t_i.

Eq. (2) implies that the scale formed during the initial stage, contributes by limiting the kinetics at the steady state for $t > t_i$. By contrast, Eq. (3), which is more commonly encountered, corresponds to the initial growth of a poorly protective oxide scale, while the steady state parabolic kinetics may be attributed to the formation of a continuous and adherent protective scale. In this case, the initial scale with mass gain Δm_i does not contribute to the control of the steady state rate.

But, as recently pointed out by Levy et al. [22], the apparent k_p determined by the slope of a Δm^2 vs t plot following the transient period, differs from the true parabolic rate constant k_p for the growth of the protective oxide scale. Thus, a determination of the true steady state parabolic rate constant by means of such parabolic plots is difficult.

According to Pieraggi [23] the plot of the kinetics data as Δm vs $t^{1/2}$ is inherently superior to the Δm^2 vs t plot for the determination of a parabolic rate constant for the steady state parabolic behavior following some faster transient growth of an initial scale.

The scale-growth kinetics could also be interpreted by using a more general expression [24]

$$t = a + b\,\Delta m + c\,\Delta m^2 \quad (4)$$

where Δm is the weight gain per unit area and t is time. In this equation the coefficient c is equal to the reciprocal of the parabolic rate constant k_p. The main advantage of Eq. (4), is that it could be fitted to the entire set of $(t, \Delta m)$ data to get a global value of k_p. Moreover, Eq. (4) could also be fitted only to a smaller part of $(t, \Delta m)$ data, to determine the local and instantaneous k_p values, representative of given time or scale thickness intervals.

The definition of an instantaneous k_p, and its variation with time, has been considered by several authors [25–27] to explain apparent discrepancies occurring between observed experimentally and purely parabolic growth kinetics. Such discrepancies are often observed for relatively short-term exposures, for which many factors may affect scaling kinetics. Some of these factors, such as the variation of diffusion coefficients within the scale, as a function of oxide grain size or scale composition, are inherent to the growing scale, but heating procedure, surface preparation and specimen handling are also known to drastically influence the first stage of scale growth. For example, these factors are of great importance for the oxidation of alloys, for which a transient stage occurs before the steady state growth of a continuous scale of the most stable oxide (for example, transformations of metastable forms of alumina into the stable a-alumina, or a change of the alloy composition below the oxide scale. Furthermore, the interfacial-reaction steps associated with mass or defect transfer at the gas–scale and/or scale–alloy interfaces, may, at least partially, contribute to the control of scale growth [28–30].

3.4. Kinetics

The results of the isothermal study are summarized in the plots of Fig. 4. The curves observed are rather smooth. The oxidation progress in every temperature follows the predictions made earlier, e.g. oxidation is much more intense at 950 °C, while in every case the phenomenon is impeded as the exposure time increases.

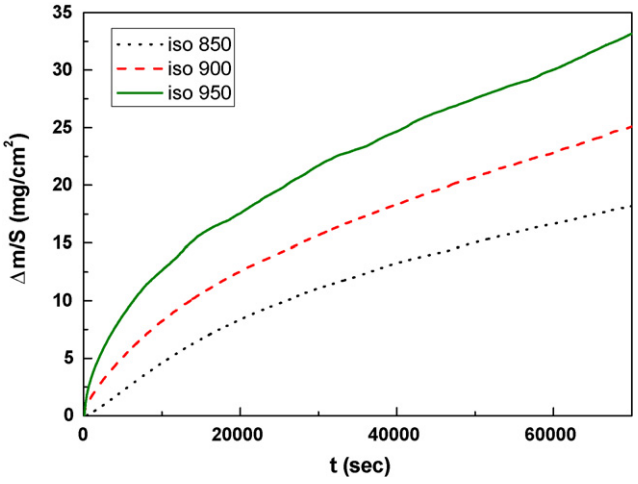

Fig. 4. Evolution of the mass gain per unit area ($\Delta m/S$) as a function of the oxidation time (t) for three different isothermal temperatures.

From these plots, the Δm–t function is possible to be estimated, along with the rate constant k_p. Three different models were used for this estimation, which included the simple correlations Δm^2 vs t and Δm vs $t^{1/2}$ and the more complicated Eq. (4).

If the simple parabolic function Δm^2 vs t is used, Fig. 5a summarizes the results at 850 °C. This plot indicates that the main part of the curve could be described with reasonable accuracy by a straight line and hence the initial assumption is true at least for this part of the curve. The deviation from this behavior, which is observed for low heating time, could be explained by assuming that, initially, a transient oxidation takes place which, after a certain exposure period, forms a stable scale. Diffusion through this scale is the controlling step and hence the mass change rate becomes parabolic. The same conclusions are also drawn when the data of Fig. 4 are presented as different functions (Δm vs $t^{1/2}$ and Eq. (4)). The plots that arise after this processing are presented in Fig. 5b and c, respectively.

In a similar way, the data were analysed for experiments performed at 900 and 950 °C. Fig. 6 presents a characteristic plot as an example of fitting with Eq. (4). This plot was added to show the differences between different temperatures. In these cases the parabolic behavior starts at a shorter time and, hence, the agreement between the theoretical parabolic law and the experimental results is much better. Consequently, the transient period is shorter, which means that the formation of the stable scale is accomplished faster with regard to the phenomena observed at 850 °C. This behavior is not peculiar, if we take into account that at a higher temperature the oxidation rate is higher.

From the above-presented oxidation-rate measurements, the values of the rate constant k_p could be calculated (for the parabolic part of the curve). The results are summarized in Table 2. As Table 2 shows, the results are very close regardless the law used. This means that the behavior of the function is very close to parabolic. Furthermore, as it was expected, the value of the rate constant increases as the oxidation temperature increases. Obviously, oxidation is more intense at higher temperature.

As it was already mentioned, k_p summarizes the effect of the factors that influence oxidation apart from time. Among these factors are included the oxidation temperature, the composition of the substrate and the mechanism of the chemical reactions that take place. For these factors the formulation of equations predicting Δm is difficult, as their effect is complicated. However, the Arrhenius law could be used. According to Arrhenius equation, the parabolic rate constant of oxidation was found to be an exponential function

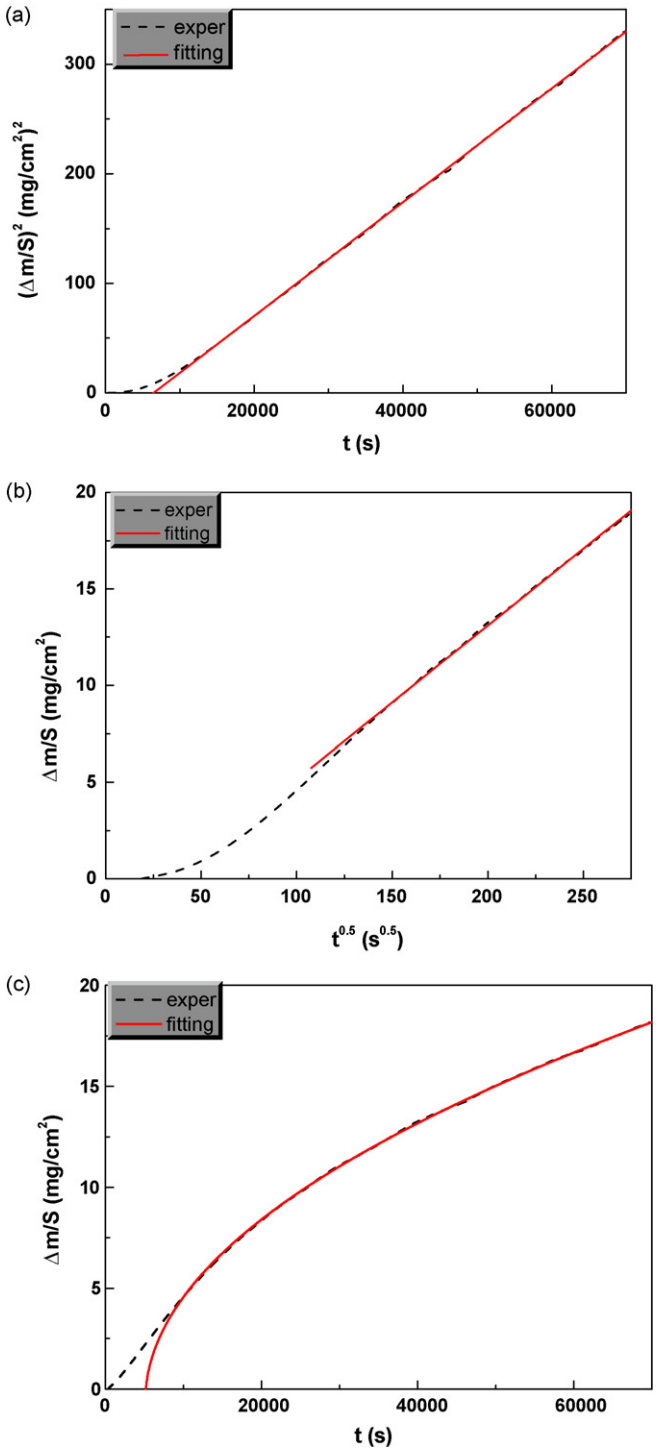

Fig. 5. (a) Mass gain per unit area $(\Delta m/S)^2$ as a function of time during oxidation obtained at 850 °C. (b) Mass gain per unit area $(\Delta m/S)$ as a function of square root of time during oxidation obtained at 850 °C. (c) Mass gain per unit area $(\Delta m/S)$ as a function of time during oxidation obtained at 850 °C.

of temperature:

$$k_p = k_o \exp\left(\frac{-E}{RT}\right) \quad (5)$$

where k_o is the pre-exponential factor, E is the apparent activation energy, R is the gas constant and T is the absolute temperature. The curve of the natural logarithm of k_p vs $1000/T$ for the values of k_p from Eq. (2) is shown in Fig. 7. From this diagram E could be calculated. The results are summarized in Table 3. The determined values are very similar to one another, as the initial data (k_p) were very close between themselves. This result shows that all three methods used for the calculation of k_p could be applied quite well to the examined experiments.

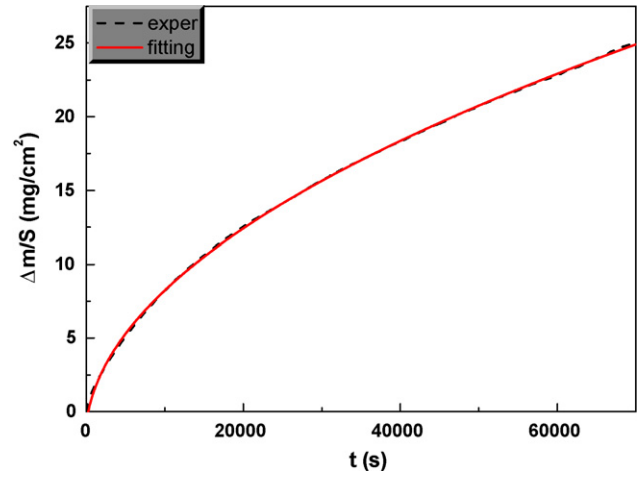

Fig. 6. Mass gain per unit area $(\Delta m/S)$ as a function of time during oxidation obtained at 900 °C.

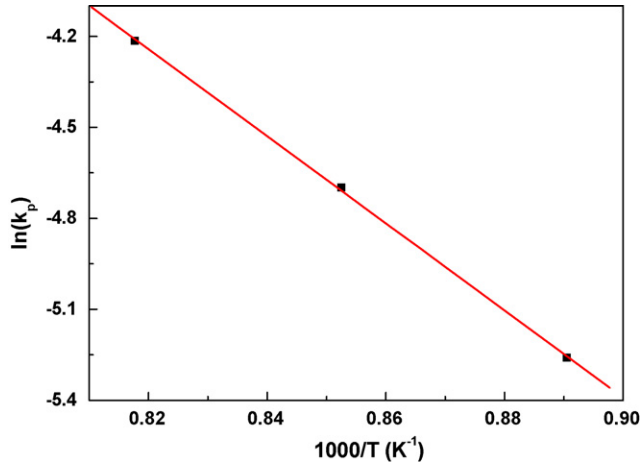

Fig. 7. Dependence of the parabolic rate constant of oxidation of the temperature.

Table 2
The values of the rate constant k_p calculated using three different expressions at three isothermal temperatures[a]

Temperature (°C)	k_p from Δm^2 vs t	k_p from Δm vs $t^{1/2}$	k_p from $t = a + b\,\Delta m + c\,\Delta m^2$
850	5.19×10^{-3}	6.4×10^{-3}	5.41×10^{-3}
900	9.09×10^{-3}	1.04×10^{-2}	1.03×10^{-2}
950	1.48×10^{-2}	1.44×10^{-2}	1.38×10^{-2}

[a] The regression factors are greater than 0.9996.

Table 3
The values of the activation energy calculated using three different expressions

Equation	Activation energy E (kJ mol^{-1})	Regression factor
Δm^2 vs t	119.6	0.9998
Δm vs $t^{1/2}$	92.7	0.9960
$t = a + b\,\Delta m + c\,\Delta m^2$	107.4	0.9900

All the above calculations were accomplished by considering a scale composed by a single oxide. In fact, the actual results that were obtained suggest such a description to be adequate. However, the EDS and XRD examinations of the oxidized samples showed a multilayered oxide scale and the existence of several metal–oxygen compounds such as Fe, Mn, Mo and Cr oxides [21], as it was already mentioned. Furthermore temperature seems to affect the thickness of the different oxide layers.

This observed oxide scale structure in accordance with the kinetics observed, which refers to a single compound. This disagreement could be explained considering that only one oxide is predominant and grows during oxidation while, the rest after an incubation period, form thin layers and afterwards their growth ceases. This means that, in fact, during oxidation only one of the steel elements reacts with oxygen. In this case the scale would be composed by a thick layer of the predominant oxide, while other oxide phases would be scattered in the mass of the main oxide, because for the oxidation progress it is necessary that diffusion takes place through their mass.

Results shown in Figs. 2 and 3 do not support this hypothesis. Another possible explanation could be developed if we considered that the growth rate of different oxides is almost the same. Of course, Fe oxides are predominant, as Fe is the main constituent of the examined substrate. For the rest of the oxides, their distribution in the mass of the Fe oxides could be attributed to diffusion in solid state, as the temperature of the system (scale–steel) remains high. This means that high temperature is not only responsible for oxidation, but it also causes changes in the already formed scale as it triggers the migration of the formed compounds .

The values which were calculated for the constant k_p and the activation energy E, could not be directly compared to the literature data for individual metal oxides. As a matter of fact, they represent the PH steel oxidation, which includes formation and growth of all the compounds detected.

4. Conclusions

The oxidation of the PH steel is negligible up to about 800 °C. Above this temperature the oxidation is intensified and results in the formation of a thick scale. This scale is composed of different layers corresponding to oxides of the main compounds of the substrate. Of course, Fe oxides are predominant, while the other metal oxides are present at lower concentrations. Furthermore the distribution in the layers is not uniform but the oxides of the minor elements (such as Mn and Mo) seem to be gathered in certain layers. The increase of the temperature does not affect the composition of the scale. However the thickness of each zone is altered.

The kinetic study reveals that oxidation is impeded as the exposure time increases. Indeed, the rate of the scale growth, as it is expressed by the increase of the substrate mass per unit area vs time, decreases at longer time of exposure. Nevertheless, the mathematical analysis of the collected data shows that a parabolic law can be used for the oxidation modelling.

The results of the kinetic calculations show that the values obtained described oxidation as if the scale was composed only by a single oxide. Hence, the equations derived and the constants that were calculated represent the overall phenomenon and not the formation of each compound separately.

References

[1] M.G. Fontana, Corrosion Engineering, 3rd ed., McGraw-Hill, New York, 1986.
[2] P. Kofstad, High Temperature Corrosion, Elsevier, London, New York, 1988.
[3] N. Birks, G.H. Meier, Introduction to High Temperature Oxidation of Metals, Edward Arnold, London, 1983.
[4] F.S. Pettit, J.B. Wagner Jr., Acta Metall. 12 (1964) 35–40.
[5] C. Wagner, Z. Phys. Chem. B21 (1933) 25.
[6] L. Himmel, R.F. Mehl, C.E. Birchenall, J. Met. Trans. AIME June (1953) 827–843.
[7] M.H. Davies, M.T. Simnad, C.E. Birchenall, J. Met. Trans. AIME October (1951) 889–896.
[8] P. Kofstad, High Temperature Corrosion, University of Oslo, Norway, 1988.
[9] R.C. Longani, W.W. Smeltzer, Can. Metall. Quart. 10 (1971) 149–163.
[10] P. Kofstad, S. Espevik, J. Electrochem. Soc. 112 (1965) 153–160.
[11] H.-J. Selenz and F. Oeters, Report from the Institute of Metallurgy (Ferrous Metallurgy) of Berlin Technical University; the Publication is part of Dr. Ing thesis, 1984.
[12] Von A. Rahmel, Werkst. Korros. 23 (1972) 95–98.
[13] Von J. Deich, F. Oeters, Werkst. Korros. 24 (1973) 365–371.
[14] C. Yan, F. Oeters, Steel Res. 65 (1994) 355–361.
[15] R. Longani, W.W. Smeltzer, Oxid. Met. 1 (1969) 3–21.
[16] Von H.-J. Grabke, Ber. Bunsen. 69 (1965) 48–57.
[17] F. Pettit, R. Yinger, J.B. Wagner Jr., Acta Metall. 8 (1960) 617–623.
[18] W.W. Smeltzer, Acta Metall. 8 (1960) 377–383.
[19] L.A. Morris, W.W. Smeltzer, Acta Metall. 15 (1967) 1591–1596.
[20] J.R. Davis (Ed.), Heat-Resistant Materials, ASM International, New York, 1997.
[21] G. Vourlias, N. Pistofidis, El. Pavlidou, K. Chrissafis, J. Therm. Anal. Calorim., accepted for publication.
[22] M. Levy, P. Farrell, F. Pettit, Corrosion 42 (1986) 708.
[23] B. Pieraggi, Oxid. Met. 27 (1987) 177–185.
[24] B. Pieraggi, R.A. Rapp, J. Electrochem. Soc. 140 (1993) 2844.
[25] A. Atkinson, R.I. Taylor, A.E. Hughes, in: R.A. Rapp (Ed.), Oxidation by Grain Boundary Diffusion: A Quantitative Demonstration of the Mechanism, NACE 6, High Temperature Corrosion, San Diego, CA, 1981, p. 110.
[26] D. Caplan, M.J. Graham, M. Cohen, J. Electrochem. Soc. 119 (1972) 1205.
[27] M.J. Graham, D. Caplan, M. Cohen, J. Electrochem. Soc. 119 (1972) 1265.
[28] U.R. Evans, Trans. Electrochem. Soc. 46 (1924) 247.
[29] B.E. Deal, A.S. Grove, J. Appl. Phys. 36 (1965) 3770.
[30] T.G. Tammann, Z. Anorg. Chem. 111 (1920) 78.